HHS Public Access

Author manuscript

Science. Author manuscript; available in PMC 2015 July 07.

Published in final edited form as:

Science. 2015 June 5; 348(6239): 1160–1163. doi:10.1126/science.aaa1356.

A Werner syndrome stem cell model unveils heterochromatin alterations as a driver of human aging

Weiqi Zhang[1,†], **Jingyi Li**[2,†], **Keiichiro Suzuki**[3,†], **Jing Qu**[4,†], **Ping Wang**[1], **Junzhi Zhou**[1], **Xiaomeng Liu**[2], **Ruotong Ren**[1], **Xiuling Xu**[1], **Alejandro Ocampo**[3], **Tingting Yuan**[1], **Jiping Yang**[1], **Ying Li**[1], **Liang Shi**[6], **Dee Guan**[1], **Huize Pan**[1], **Shunlei Duan**[1], **Zhichao Ding**[1], **Mo Li**[3], **Fei Yi**[5], **Ruijun Bai**[4], **Yayu Wang**[6], **Chang Chen**[1], **Fuquan Yang**[1], **Xiaoyu Li**[7], **Zimei Wang**[8], **Emi Aizawa**[3], **April Goebl**[3,9], **Rupa Devi Soligalla**[3], **Pradeep Reddy**[3], **Concepcion Rodriguez Esteban**[3], **Fuchou Tang**[2,10,11,12,*], **Guang-Hui Liu**[1,8,11,13,*], and **Juan Carlos Izpisua Belmonte**[3,*]

[1]National Laboratory of Biomacromolecules, Institute of Biophysics, Chinese Academy of Sciences, Beijing 100101, China

[2]Biodynamic Optical Imaging Center, College of Life Sciences, Peking University, Beijing 100871, China

[3]Gene Expression Laboratory, Salk Institute for Biological Studies, 10010 North Torrey Pines Road, La Jolla, California 92037, USA

[4]State Key Laboratory of Reproductive Biology, Institute of Zoology, Chinese Academy of Sciences, Beijing 100101, China

[5]Department of Molecular and Cellular Physiology, Stanford University School of Medicine, Stanford, California 94305, USA

[6]Diagnosis & Treatment Center for Oral Disease, the 306th Hospital of the PLA

[7]College of Life Sciences, Peking University, Beijing 100871, China

[8]The Center for Anti-aging and Regenerative Medicine, Shenzhen University, Shenzhen 518060, China

[9]Universidad Católica San Antonio de Murcia, Campus de los Jerónimos s/n, 30107 Guadalupe, Murcia, Spain

[10]Ministry of Education Key Laboratory of Cell Proliferation and Differentiation, Beijing 100871, China

[11]Center for Molecular and Translational Medicine, CMTM, Beijing 100101, China

[12]Peking-Tsinghua Center for Life Sciences, Peking University, Beijing 100871, China

[*]Correspondence: belmonte@salk.edu (JCIB), ghliu@ibp.ac.cn (GHL), or tangfuchou@pku.edu.cn (FT).
[†]These authors contributed equally to this work

Supplementary Materials
Material and Methods
Figs. S1 to S11
Table S1 to S5

[13]Beijing Institute for Brain Disorders, Beijing 100069, China

Abstract

Werner syndrome (WS) is a premature aging disorder caused by WRN protein deficiency. Here, we report on the generation of a human WS model in human embryonic stem cells (ESCs). Differentiation of WRN-null ESCs to mesenchymal stem cells (MSCs) recapitulates features of premature cellular aging, a global loss of H3K9me3, and changes in heterochromatin architecture. We show that WRN associates with heterochromatin proteins SUV39H1 and HP1α and nuclear lamina-heterochromatin anchoring protein LAP2β. Targeted knock-in of catalytically inactive *SUV39H1* in wild-type MSCs recapitulates accelerated cellular senescence, resembling WRN-deficient MSCs. Moreover, decrease in WRN and heterochromatin marks are detected in MSCs from older individuals. Our observations uncover a role for WRN in maintaining heterochromatin stability and highlight heterochromatin disorganization as a potential determinant of human aging.

Werner syndrome (WS), also known as adult progeria, recapitulates certain aspects of human physiological aging (1). WS is caused by mutations in the *WRN* gene resulting in loss of WRN expression or function (1). WRN protein plays roles in DNA replication, transcription, repair, recombination as well as telomere maintenance, indicating that one of the major causes for WS pathogenesis relates to genomic instability (1, 2). Epigenetic alterations have been associated with cellular aging in diverse model organisms (2–4). In humans, somatic cells derived from patients with premature aging syndromes are characterized by loss of heterochromatin marks (5–7). However, it is unclear whether epigenetic dysregulation is involved in WS pathogenesis.

Generation of patient-specific pluripotent stem cells represents a promising avenue to model and study human aging and aging-associated disorders (8). WS-specific iPSCs lines may constitute an ideal source for in vitro modeling of WS. However, we found that WS patient fibroblast lines deposited in different cell banks presented severe karyotypic abnormalities and secondary DNA mutations associated with advanced stages of WS pathology. To create an unbiased human WS cellular model, we sought to generate an isogenic WS ESC line by knocking out exons 15 and 16 of the *WRN* gene encoding for the conserved DNA helicase domain (9). Following two rounds of homologous recombination using helper-dependent adenoviral vector (HDAdV) (10, 11), we successfully generated homozygous *WRN* null ESC lines (ESCs-$WRN^{-/-}$) (Fig. 1A, B and fig. S1A–D). ESCs-$WRN^{-/-}$ expressed pluripotency markers, maintained normal karyotype and were able to differentiate into all three germ layers (Fig. 1A and fig. S2A–E). ESCs-$WRN^{-/-}$ lacked detectable WRN protein, as determined by Western blot using antibodies specific to the amino or carboxyl terminus of WRN (Fig. 1B). No difference in cell cycle kinetics and cell growth rate between wild-type and WRN-null ESCs was observed (fig. S2F–H).

WS patients are mainly characterized by premature aging pathologies associated with degeneration of mesodermal tissues, i.e. osteoporosis, atherosclerosis and grey hair (1). We hypothesized that WS patients may suffer from an accelerated exhaustion of the MSC pool. This was tested by differentiating ESCs-$WRN^{-/-}$ into MSCs. MSCs-$WRN^{-/-}$ expressed MSC-specific cell surface markers CD73, CD90, CD105, lacked expression of MSC-

irrelevant antigens including CD45, CD34 and CD43 (fig. S3A), and were able to differentiate towards osteoblasts, chondrocytes, and adipocytes (fig. S3B, C) (12).

Upon serial passaging, WRN-deficient MSCs recapitulated major phenotypes of premature aging, including premature loss of proliferative potential, increased number of senescence-associated-β-galactosidase (SA-β-gal) positive cells, upregulated expression of aging-associated genes $p16^{Ink4a}$ and $p21^{Waf1}$, and activation of senescence-associated secretory phenotype (SASP) (Fig. 1C–E and fig. S3D–G) (13). Moreover, when WRN-deficient MSCs expressing luciferase were transplanted into the muscle of NOD/SCID mice, they underwent an accelerated attrition compared to wild type MSCs (Fig. 1F and fig. S3H). These results demonstrated that the loss of WRN promotes premature senescence in MSCs.

WRN deficiency in MSCs resulted in elevated DNA damage response (DDR), indicated by increased nuclear foci for 53BP1, γ-H2AX and phosphorylated ATM/ATR substrates (fig. S4A–C). Restoration of WRN activity by lentivirus-mediated expression in MSCs-$WRN^{-/-}$ resulted in partial alleviation of DDR and cellular senescence (fig. S4D, E). To investigate potential chromosomal abnormalities resulting from the loss of WRN protein, we performed genome-wide copy number variation (CNV) analysis by deep sequencing. In the time frame examined, genomic integrity was minimally affected in MSCs-$WRN^{-/-}$ (fig. S4F).

Epigenetic alteration has been postulated as a driver of aging (2). MSCs-$WRN^{-/-}$ showed a distinct nuclear Hoechst 33342 staining pattern with markedly enlarged nuclei and high pixel-to-pixel coefficient of variation (C.V.) value, indicating possible changes in chromatin structure (Fig. 2A and fig. S5A). Moreover, WRN-deficient MSCs exhibited accelerated diminishment of heterochromatin-associated inner nuclear membrane (INM) proteins LAP2β and LBR, and reduced heterochromatin structure underneath the nuclear envelope, as indicated by immunostaining and electron microscopy (Fig. 2B and fig. S5B, C) (14). These results suggest a progressive disorganization of heterochromatin in WRN-deficient MSCs.

Further investigation of heterochromatin reorganization at histone and DNA levels revealed significant downregulation of the constitutive heterochromatin mark H3K9me3 in MSC-$WRN^{-/-}$ (Fig. 2C and fig. S5D, E). In contrast, H3K27me3 showed slight downregulation, while H3K4me3, a mark for euchromatin fiber, exhibited comparable levels between WRN-deficient and wild-type MSCs (Fig. 2C and fig. S5D, E). We did not observe significant genome-wide alteration of 5mC in WRN-deficient MSCs (Fig. 2C). Bioinformatic analysis identified 73 H3K9me3-enriched “mountains” throughout the genome in MSCs-$WRN^{+/+}$, which are characterized by over 20 kb of consecutive peaks of H3K9me3 (Fig. 2D). 28 (38%) of these H3K9me3 mountains were lost in MSCs-$WRN^{-/-}$ (Fig. 2D). Interestingly, 24 (86%) of these impaired H3K9me3 mountains resided in sub-telomeric or sub-centromeric regions (Fig. 2E and Table S1).

RNA-seq identified 1,047 RefSeq genes that showed differential expression in MSCs-$WRN^{-/-}$ (Table S2). The most significantly down-regulated genes were centromere-packaging proteins and components of the nuclear membrane (fig. S6A–E and Table S3). These results indicate alterations in nuclear structure and epigenomic organization

potentially leading to a progressive loss of heterochromatin structure in MSCs as a consequence of WRN depletion.

In agreement with previous reports describing WRN as a telomere-associated protein required for telomere maintenance (15), compromised telomerase activity and shorter telomere length was detected in MSC-*WRN*$^{-/-}$ (fig. S7A, B). In addition, quantitative ChIP-PCR (ChIP-qPCR) showed binding of WRN to the H3K9me3-enriched centromeric loci α-Satellite (α-Sat) and Satellite 2 (Sat2) (Fig. 3A) (16). Depletion of WRN resulted in an increase in centromeric γ-H2AX signal and a loss of H3K9me3 from α-Sat and Sat2 loci accompanied by upregulation of transcripts from these sequences (Fig. 3A, B and fig. S7C). Co-immunoprecipitation (Co-IP) analysis revealed WRN as part of a complex containing the major histone methyltransferase for H3K9me3 - SUV39H1, HP1α, and LAP2β, a nuclear envelope component that recruits heterochromatin via anchoring to HP1α (Fig. 3C and fig. S7D) (17). These observations suggest a role for WRN, together with SUV39H1 and HP1α, in the stabilization of heterochromatin.

We next tested whether disorganization of heterochromatin could contribute to accelerated cellular senescence. Knockdown of SUV39H1 or HP1α in wild-type MSCs led to a significant reduction of overall H3K9me3 and induction of cellular senescence, as assayed by Western blot, SA-β-gal staining, and p16 expression (Fig. 3D and fig. S8A–D). On the contrary, overexpression of HP1α upregulated H3K9me3 levels and repressed cellular senescence in WRN-deficient MSCs (fig. S8E–H). To confirm these observations, we generated pluripotent ESCs-*SUV39H1*^{H324K} lines harboring catalytically inactivated endogenous SUV39H1 (fig. S9A–D). Upon differentiation, MSCs-*SUV39H1*^{H324K} displayed drastic nuclear structural and chromosomal changes, loss of INM proteins LAP2β and LBR, decreased levels of H3K9me3 and HP1α, upregulation of centromeric repetitive sequence transcription, and coordinated transcriptional downregulation of centromere-packaging components (Fig. 4A–C and fig. S10A, B). MSCs-*SUV39H1*^{H324K} recapitulated premature aging phenotypes observed in WRN deficient MSCs, including retarded cell growth and accelerated cellular senescence determined by SA-β-gal staining (Fig. 4D and fig. S10C–E). High expression of SUV39H2, a germline-specific histone methyltransferase, and/or other factors may functionally compensate for SUV39H1 deficiency in ESCs (fig. S10F) (18, 19), where upon inactivation of the WRN-SUV39H1 axis, no discernible heterochromatin change was observed (fig. S10G and S8A). It should be noted that MSCs-*SUV39H1*^{H324K} exhibit neither increased γ-H2AX ($P=0.773$) and phosphorylated ATM/ATR substrates ($P=0.279$), nor telomere attrition (fig. S10H and S7A, B). These results indicate that active heterochromatin destabilization promotes premature aging in MSCs.

Finally, we asked whether heterochromatin disorganization could be a common hallmark for physiological human stem cell aging. For this purpose, we compared the levels of heterochromatin marks in primary dental pulp MSCs derived from six young (7–26 year old) and six old (58–72 year old) individuals (fig. S10I, and Table S4) (20). A marked downregulation of WRN protein associated with a decrease in H3K9me3, HP1α, SUV39H1, and LAP2β levels in MSCs derived from old individuals (Fig. 4E). Therefore, specific

heterochromatin changes may underlie both pathological as well as physiological mesenchymal stem cell aging.

In summary, we have found that WRN protein, besides its role in DNA repair, functions to safeguard heterochromatin stability (fig. S11). Our results unveil that the progressive heterochromatin disorganization observed in WRN deficient MSCs underlies cellular aging, but more extensive studies are needed to examine its role during physiological aging. The methodologies and observations here introduced may be used and extended towards the systematical study of other age-associated molecular events with relevance to human aging and age-related disorders.

Supplementary Material

Refer to Web version on PubMed Central for supplementary material.

Acknowledgments

We are grateful to W. Zhu, L. Comai, K. Mitani, P. Ng and A. Lieber for sharing experimental materials, L. Sun, W. Ding, G. Yuan, and X. Zhu for technical assistance, and M. Schwarz for administrative help. This work was supported by National Natural Science Foundation of China (NSFC: 81330008), National Basic Research Program of China (973 Program, 2015CB964800; 2014CB910500; 2014CB964600; 2012CB966704), the Strategic Priority Research Program of the Chinese Academy of Sciences (XDA01020312), NSFC (31222039; 31201111; 81371342; 81300261; 81300677; 81271266; 81471414; 81422017; 81401159; 31322037; 81471407), Beijing Natural Science Foundation (7141005; 5142016), Key Research Program of the Chinese Academy of Sciences (KJZDEW-TZ-L05), the Thousand Young Talents program of China, National Laboratory of Biomacromolecules (012kf02;2013kf05;2013kf11;2014kf02;2015kf10), and State Key Laboratory of Drug Research (SIMM1302KF-17), and China Postdoctoral Science Foundation Grant (2013M530751). K.S and M.L. are supported by a California Institute for Regenerative Medicine Training Grant. A.O. was partially supported by an NIH Ruth L. Kirschstein National Research Service Award Individual Postdoctoral Fellowship. The physiological human cell aging studies were supported by UCAM. J.C.I.B. laboratory was supported by The Glenn Foundation, The G. Harold and Leila Y. Mathers Charitable Foundation and The Leona M. and Harry B. Helmsley Charitable Trust (2012-PG-MED002).

References and Notes

1. Kudlow BA, Kennedy BK, Monnat RJ Jr. Nat Rev Mol Cell Biol. 2007; 8:394–404. [PubMed: 17450177]
2. Lopez-Otin C, Blasco MA, Partridge L, Serrano M, Kroemer G. Cell. 2013; 153:1194–1217. [PubMed: 23746838]
3. Pegoraro G, et al. Nature cell biology. 2009; 11:1261–1267.
4. Greer EL, et al. Nature. 2010; 466:383–387. [PubMed: 20555324]
5. Liu GH, et al. Nature. 2011; 472:221–225. [PubMed: 21346760]
6. Shumaker DK, et al. Proc Natl Acad Sci U S A. 2006; 103:8703–8708. [PubMed: 16738054]
7. Miller JD, et al. Cell Stem Cell. 2013; 13:691–705. [PubMed: 24315443]
8. Liu GH, Ding Z, Izpisua Belmonte JC. Curr Opin Cell Biol. 2012; 24:765–774. [PubMed: 22999273]
9. Lombard DB, et al. Mol Cell Biol. 2000; 20:3286–3291. [PubMed: 10757812]
10. Liu GH, et al. Nature. 2012; 491:603–607. [PubMed: 23075850]
11. Suzuki K, et al. Cell Stem Cell. 2014; 15:31–36. [PubMed: 24996168]
12. Liu GH, et al. Nat Commun. 2014; 5:4330. [PubMed: 24999918]
13. Rodier F, Campisi J. J Cell Biol. 2011; 192:547–556. [PubMed: 21321098]
14. Dechat T, Adam SA, Taimen P, Shimi T, Goldman RD. Cold Spring Harb Perspect Biol. 2010; 2:a000547. [PubMed: 20826548]

15. Multani AS, Chang S. J Cell Sci. 2007; 120:713–721. [PubMed: 17314245]
16. Wang D, et al. Proc Natl Acad Sci U S A. 2013; 110:5516–5521. [PubMed: 23509280]
17. Kourmouli N, et al. Embo J. 2000; 19:6558–6568. [PubMed: 11101528]
18. O'Carroll D, et al. Mol Cell Biol. 2000; 20:9423–9433. [PubMed: 11094092]
19. Zhang W, Qu J, Suzuki K, Liu GH, Belmonte JC. Trends Cell Biol. 2013
20. Tomar GB, et al. Biochem Biophys Res Commun. 2010; 393:377–383. [PubMed: 20138833]

General summary for “This Week in Science”

Study of human aging is technically challenging. It is a lengthy process and access to isogenic samples from young and old individuals is not straightforward. Patients with Werner syndrome (WS) show accelerated aging-associated features, thus providing an advantageous model to study the process of human aging. Zhang et al. have now generated, through gene editing, isogenic WS-specific human embryonic stem cell (ESC) lines. Upon differentiation, WS-mesenchymal stem cells (MSCs) displayed premature aging accompanied by heterochromatin disorganization, a phenomenon that also occurs in physiologically aging MSCs. This report establishes a novel role for WRN protein in heterochromatic maintenance and highlights heterochromatin alterations as a driving force of human aging.

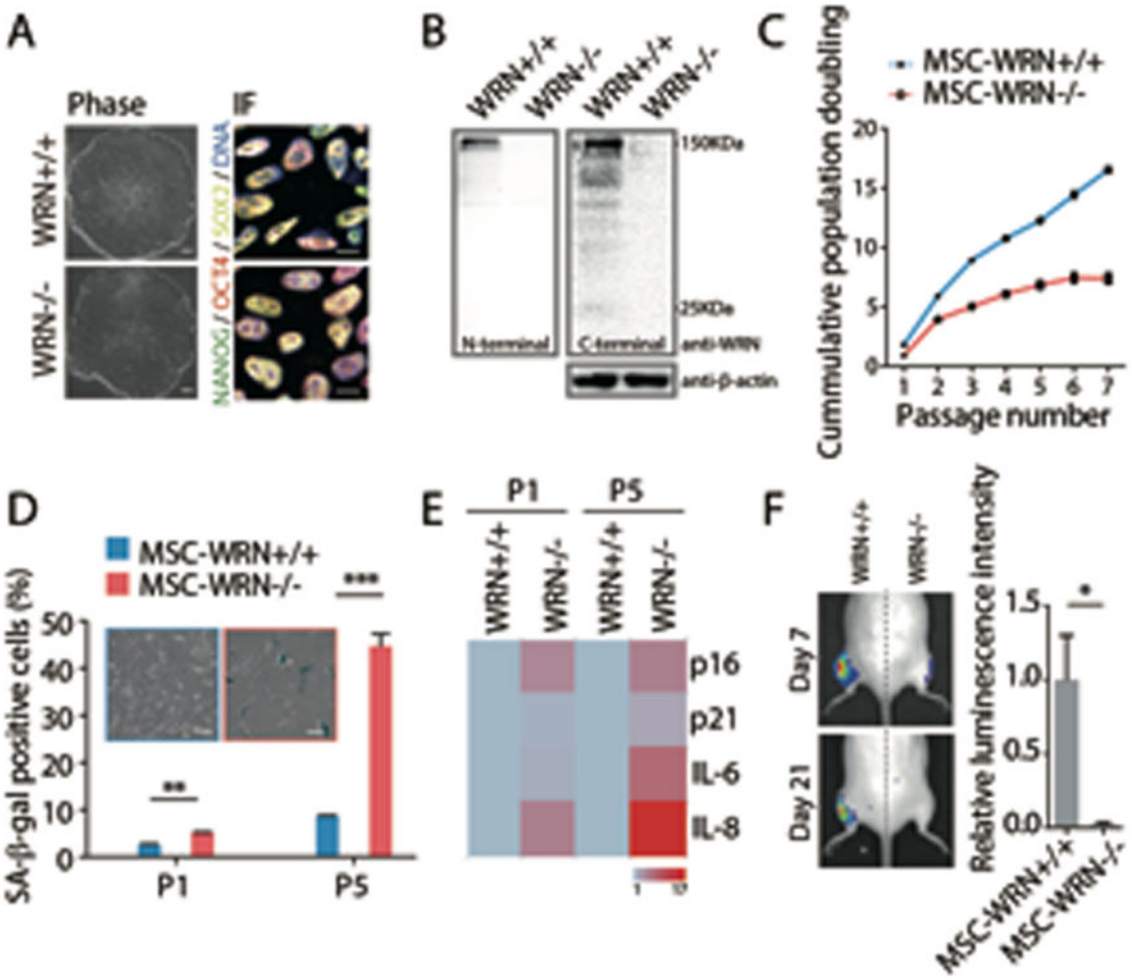

Fig. 1. WRN-deficient MSCs exhibit phenotypes associated with premature cellular senescence

(**A**) Morphology and immunofluorescence analyses of pluripotency markers in ESCs. Scale bar, 100 μm and 10 μm, respectively. (**B**) Western blot analysis of WRN expression in ESCs using anti-WRN N-terminal (ab200) and C-terminal (SC-5629) antibodies. (**C**) Growth curve analyzing the accumulative population doubling of MSCs. (**D**) Senescence-associated (SA)-β-gal staining in passage 1 (P1) and P5 MSCs. Scale bar, 50μm. (**E**) Quantitative RT-PCR analysis of the indicated genes in P1 and P5 MSCs. Transcript levels were normalized to MSCs-*WRN*$^{+/+}$ group. Genes with greater mean value are color coded towards red. (**F**) Photon flux from muscle of NOD-SCID mouse transplanted with MSCs-*WRN*$^{+/+}$ (left) and MSCs-*WRN*$^{-/-}$ (right) expressing luciferase. All data are represented as mean + SEM. *P<0.05, **P<0.01, ***P<0.001 by t test; n=3.

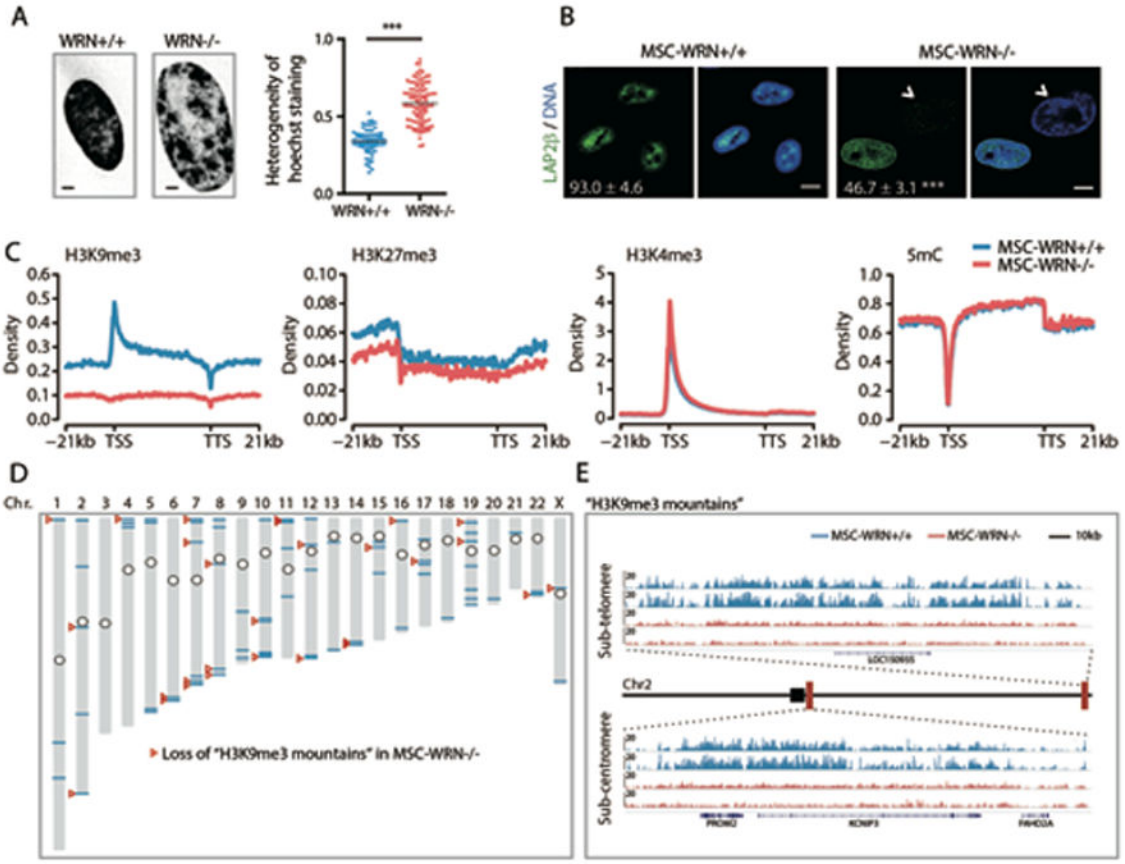

Fig. 2. Epigenomic analyses of WRN-deficient MSCs

(**A**) Left, Chromatin structure of MSCs shown by Hoechst 33342 staining of the nucleus. Scale bar, 5μm.; Right, C.V. value of nuclear Hoechst staining intensity used to evaluate the heterogeneity (pixel-to-pixel variation) of Hoechst intensity. (**B**) Immunofluorescence analyses of LAP2β expression in MSC-$WRN^{+/+}$ and MSC-$WRN^{-/-}$ at P5. Arrowheads denote abnormal nuclei with decreased LAP2β expression (percentage of LAP2β–positive nuclei in corner). Scale bar, 10 μm. (**C**) Enrichment of H3K9me3, H3K27me3, H3K4me3, and 5mC on the gene bodies and 21kb upstream of TSS and 21kb downstream of TTS regions in human genome. (**D**) Sketch map of "H3K9me3 mountain" distribution over 23 chromosomes. The blue lines indicate 73 "H3K9me3 mountains" present in MSCs-$WRN^{+/+}$ whereas 48 (65.8%) of them are localized within 5 Mb regions around the telomeres or centromeres. The red arrowheads indicate 28 "H3K9me3 mountains" which are lost in MSCs-$WRN^{-/-}$. The circles indicate the centromeres of chromosomes. (**E**) Representative images showing two "H3K9me3 mountains" on chromosome 2 in the sub-telomere or sub-centromere regions in P5 MSCs-$WRN^{-/-}$ and MSCs-$WRN^{+/+}$. Two biological replicates of each sample are presented. Black square denotes the centromere; red rectangles denote the position of the presented sub-telomere and sub-centromere regions, respectively. All data are represented as mean + SEM. ***P<0.001 by t test; n=3.

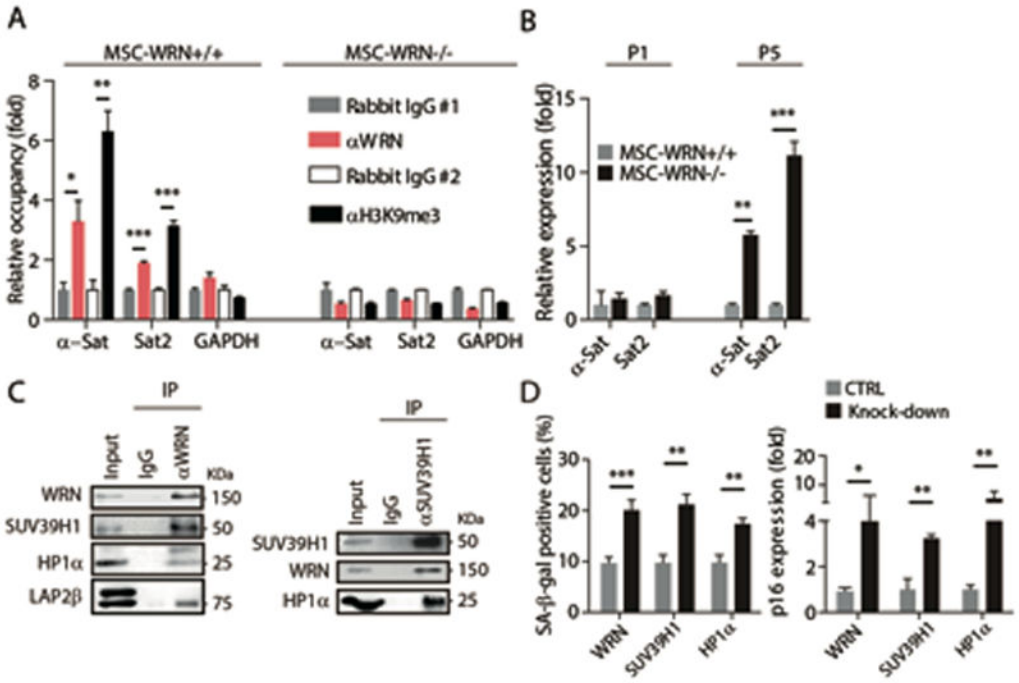

Fig. 3. WRN associates with centromeric heterochromatin, and forms a molecular complex with SUV39H1 and HP1α

(**A**) Enrichment of WRN and H3K9me3 within the region of α-Sat or Sat2 as measured by ChIP-qPCR. (**B**) Quantitative RT-PCR analysis of centromeric repetitive element transcripts in MSCs at the indicated passages. (**C**) Left, co-immunoprecipitation of SUV39H1, HP1α, and LAP2β protein with endogenous WRN protein; Right, co-immunoprecipitation of WRN and HP1α with endogenous SUV39H1 in wild-type MSCs. (**D**) SA-β-gal staining (left) and p16 transcript (right) analyses in wild-type MSCs transduced with control lentiviral vector (CTRL) or lentiviral vector encoding for the indicated shRNA (Knock-down). All data are represented as mean + SEM. *P<0.05, **P<0.01, and ***P<0.001 by t test; n=3.

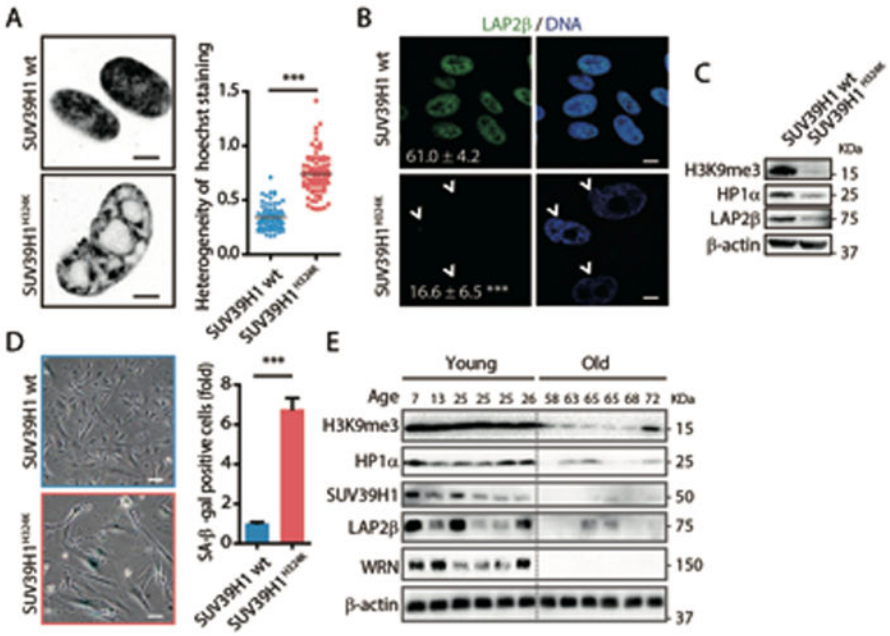

Fig. 4. *SUV39H1*^{H324K} mutant MSCs exhibit defective nuclear envelope and heterochromatin, as well as phenotypes of premature cellular senescence

(**A**) As described in Fig 2A, Left, Hoechst staining images of the nucleus; Right, C.V. value of nuclear Hoechst staining intensity used to evaluate the heterogeneity (pixel-to-pixel variation) of Hoechst intensity. (**B**) Immunofluorescence analyses of LAP2β expression in MSCs. Arrowheads denote the abnormal nuclei with decreased LAP2β (Percentages of normal nuclei presented at corner). Scale bar, 20 μm. (**C**) Western blot analysis of the indicated proteins in MSCs. (**D**) SA-β-gal staining in MSCs at P5. Scale bar, 50 μm. (**E**) Western blot analysis of the indicated proteins in human primary MSCs derived from old and young healthy individuals at P4 (see Table S4). All data are represented as mean + SEM. *P<0.05, ***P<0.001 by t test; n=3.